ALTIUS: a spaceborne AOTF-based UV-VIS-NIR hyperspectral imager for atmospheric remote sensing

Emmanuel Dekemper[a], Didier Fussen[a], Bert Van Opstal[a], Jurgen Vanhamel[a], Didier Pieroux[a], Filip Vanhellemont[a], Nina Mateshvili[a], Ghislain Franssens[a], Vitaly Voloshinov[b], Christof Janssen[c,d], Hadj Elandaloussi[c,d]

[a]Belgian Institute for Space Aeronomy (IASB-BIRA), 3 avenue Circulaire, 1180 Brussels, Belgium;
[b]Lomonosov Moscow State University (MSU), Leninskie Gory, 119991 Moscow, Russian Federation;
[c]CNRS, UMR 8112, LERMA, 4 pl Jussieu, 75005 Paris, France;
[d]Sorbonne Universités, UPMC Univ Paris 06, UMR 8112, LERMA, 4 pl Jussieu, 75005 Paris, France.

ABSTRACT

Since the recent losses of several atmospheric instruments with good vertical sampling capabilities (SAGE II, SAGE III, GOMOS, SCIAMACHY, MIPAS), the scientific community is left with very few sounders delivering concentration profiles of key atmospheric species for understanding atmospheric processes and monitoring the Earth's radiative balance. The situation is so critical that, less than five such instruments will be on duty (most probably only 2 or 3) at the horizon 2020, whereas their number topped more than 15 in the years 2000. In parallel, recent inter-comparison exercises among the climate chemistry models (CCM) and instrument datasets have shown large differences in vertical distribution of constituents (SPARC CCMVal and Data Initiative), stressing the need for more accurate vertically-resolved data at all latitudes.

In this frame, the Belgian Institute for Space Aeronomy (IASB-BIRA) proposed a small mission called ALTIUS (Atmospheric Limb Tracker for the Investigation of the Upcoming Stratosphere), which is currently in preliminary design phase (phase B according to ESA standards). Taking advantage of the good performances of the PROBA platform (PRoject for On-Board Autonomy) in terms of pointing precision and accuracy, on-board processing ressources, and agility, the ALTIUS concept relies on a hyperspectral imager observing limb-scattered radiance and solar/stellar occultations every orbit. The objective is twofold: compared to scanning instruments, the imaging feature allows to better assess the tangent height of the sounded air masses (through easier star tracker information validation by recognition of scene details), while its spectral capabilities will be good enough to exploit the characteristic signatures of many molecular absorption cross-sections (O_3, NO_2, CH_4, H_2O, aerosols,...). The payload will be divided in three independent optical channels, associated to separated spectral ranges (UV: 250-450 nm, VIS: 440-800 nm, NIR: 900-1800 nm). This approach also offers better risk mitigation in case of failure of one channel. In each channel, the spectral filter will be an acousto-optical tunable filter (AOTF). Such devices offer reasonable étendue with good spectral resolution and excellent robustness and compactness and TeO_2-based AOTF's have already been used in space missions towards Mars and Venus (MEX and VEX, ESA). While such TeO_2 crystals are common in VIS-NIR applications, they are not transparent below 350 nm. Recent progresses towards UV AOTF's have been made with the advent of KH_2PO_4-based (KDP) filters. Through collaboration with the Moscow State University (MSU), several experiments were conducted on a KDP AOTF and gave confidence on this material.

Here, we present the general concept of ALTIUS and its optical design with particular attention on the AOTF. Several results obtained with optical breadboards for the UV and VIS ranges will be exposed, such as the O_3 and NO_2 absorption cross-section measurements, or spectral images. These results illustrate the spectral

Corresponding author: E. Dekemper (emmanuel.dekemper@aeronomie.be). Principal Investigator (PI) of the ALTIUS mission: D. Fussen (didier.fussen@aeronomie.be).

Sensors, Systems, and Next-Generation Satellites XVIII, edited by Roland Meynart, Steven P. Neeck, Haruhisa Shimoda, Proc. of SPIE Vol. 9241, 92410L · © 2014 SPIE
CCC code: 0277-786X/14/$18 · doi: 10.1117/12.2063937

and optical performances to be expected from an AOTF-based hyperspectral imager. Their implications for the ALTIUS mission will be discussed.

Keywords: Remote sensing, atmosphere, AOTF, hyperspectral imager

1. INTRODUCTION

After decades of steady increase of long-lived halogen chlorine and bromine compounds in the stratosphere, the Montreal protocol and its subsequent amendments have succeded in slowing down and then reversing the trend of these ozone depleting species (ODS). The generally accepted turning point is the year 1997. Nearly 20 years later, atmospheric models and ozone total column measurements agree to a weak recovery (less than 2%/decade). The current understanding explaining the slowness of progress is mainly due to radiative effects caused by increasing greenhouse gases (GHG) balancing the decrease of ODS.[1]

While the agreement is generally good among total column datasets, the situation is different for ozone profiles. Recently, Bourassa et al.[2] have merged data from SAGE-II and OSIRIS to cover the period 1984-2013 with monthly mean ozone profile time series. After 1997, they find trends larger than 5%/decade at high altitudes in the Southern mid-latitudes and still positive but smaller values for the Northern counterpart. On the other hand, no significant trend in the tropics and even negative trends of a few percents have been found in the lower stratosphere (LS) from 40°S to 40°N. While similar studies with SCIAMACHY, GOMOS or MIPAS data are in good agreement for the asymmetric behaviour from one hemisphere to the other in the upper stratosphere (US), there are discrepancies in terms of trend amplitude or even contradictions for some regions, i.e. mainly in the tropics and Northern mid-latitudes, below the ozone maximum.[3–5]

Recently, several reprocessing activities have been undertaken, namely the Stratosphere-troposphere Processes And their Role in Climate (SPARC) Data Initiative or the ozone Climate Change Initiative (O3CCI) among others. Their goal is to prepare and possibly merge datasets from various instruments in order to perform trend analyses, assess possible biases or build consistent datasets for atmospheric models. For the SPARC activity, Tegtmeier et al.[6] have shown how broad the dispersion of the measurements of 18 limb sounders can be. While most instruments agree to within ±5% for their annual-mean zonally-averaged ozone profile in the US at most latitudes (except for SCIAMACHY and ACE-FTS), the situation is worse in the LS, confirming the difficulties to obtain a global picture of the ozone field from past and current atmospheric profilers.

Accurate high-resolution concentration profiles can only be provided by instruments looking tangentially to the atmospheric limb. There are essentially three families of limb sounders with specific advantages and drawbacks. Their working principle relies on (1) the occultation of celestial bodies (Sun, stars, planets, moon), (2) the limb-scattered solar radiance, and (3) the thermal emissions by atmospheric constituents. Independently of the measurement technique, limb sounders are sensitive to one particular aspect: the knowledge of their line of sight tangent height. With typical ozone profiles showing steep gradients above and below the ozone maximum, pointing errors of a few hundred meters easily yield biases larger than 10%.[7] In light of the discussion on the trends in ozone recovery, the minimization of tangent height uncertainties is a crucial target, certainly a driver for new instruments.

In the following sections, we present a new UV-VIS-NIR multi-mode (limb-scattering and occultation) instrument for the remote sensing of ozone profiles and other important stratospheric species which is currently in a preliminary design phase (phase B). We will focus on several key aspects such as the tunable spectral filters or the solutions retained for dealing with the high dynamic scale of the observed scene (the bright limb). The expected instrument performance will be illustrated by experimental results.

2. THE ALTIUS MISSION

ALTIUS is a small mission (in terms of cost and volume) whose primary goal is to provide accurate ozone concentration profiles from the upper troposphere (12-15 km) up to the lower mesosphere (≈60 km) with a relatively high geographical sampling. Secondary objectives include nitrogen dioxide, aerosols, polar stratospheric and noctilucent clouds, methane and water vapor. Therefore the ALTIUS instrument will be inserted on a sun-synchronous low-Earth orbit (LEO) with an ascending node at 10:30 AM. During the dayside of the orbit, it will

perform limb-scatter measurements. At the terminator, it will follow the sunset (solar occultation) and continue in the dark side with stellar/lunar/planetary occultations. Back in the penumbra, a new solar occultation is performed (sunrise) and the full sequence is repeated. The PROBA platform will be used as it offers good attitude control[8] and manœuvrability. The three PROBA satellites — PROBA-1, PROBA-2 and PROBA-V launched in 2001, 2009 and 2013 respectively — have proved to be reliable systems as all three are still operating nominal.

A possible choice for a small mission targetting ozone is to rely on its strong absorption in the UV and VIS domain to infer abundance. In this range, passive remote sensing instruments use the Sun as a light source either by looking at its transmittance (solar occultation), either by measuring the solar limb-scattered radiance. The solar occultation technique delivers high-resolution profiles (typically 1 km) but suffers from a poor coverage (two events per orbit). The limb scattering technique has a much broader coverage, but the vertical resolution is slightly coarser (2-3 km) and the determination of the tangent height of the line of sight is more complex. These figures have been reported by previous instruments and do not constitute fundamental limitations. One purpose of ALTIUS is to make them smaller.

Most of the instruments with limb-scattering capabilities (OSIRIS, SCIAMACHY, SAGE-III, GOMOS) have been based on grating spectrometers coupled to a scanning (or tracking in the case of GOMOS) system to cover the vertical range of interest. One exception is the currently flying OMPS-LP instrument onboard the SNPP platform. It uses a prism and vertical slits which capture the radiance profile at once. However, all instruments have used methods based on spectral radiance or ozone profile fitting[9–11] to assess their pointing knowledge. Generally, a precision of 350-500 m is reached with this technique.

While ALTIUS will be capable of using a similar technique for cross-checking, its main tangent altitude registration strategy is twofold. First, the PROBA attitude and orbit control system (AOCS) has demonstrated[8] with PROBA-2 a pointing jitter smaller than 5 arcsec (2σ confidence level). This corresponds to an uncertainty (2σ) of 70 m at the tangent point. Second, the ALTIUS concept is based on a spectral imager taking monochromatic snapshots of the limb. At its highest resolution, the digital frames will sample a 100×100 km^2 scene with 512×512 pixels. Hence, calibration strategies based on the identification of two or more stars in the field of view (FOV) will allow to validate the AOCS information independently. This method alone will bring the uncertainty below 200 m at least, i.e. the image resolution.

This unprecedented high measurement sampling also plays a role in the expected high vertical resolution of the retrieved ozone profiles. Discussing ALTIUS level-2 products quality is beyond the scope of this paper, but simulations show that in the case of ozone, the bright limb data will allow to meet the vertical resolution (the spacing between independent pieces of information) usually achieved by the occultation technique, i.e. typically 1 km.

2.1 High Dynamic Range Sensors

Owing to Rayleigh scattering, the limb radiance profile is governed by the air density profile. Independently of the wavelength of acquisition, the flux of photon will decrease by 3 to 4 orders of magnitude from the upper troposphere to the lower mesosphere (Fig. 1). Scanning instruments change their detector gain and integration times step-wise to deal with this high dynamic range. True imagers like ALTIUS must employ a different approach to avoid saturation of the lower part of the scene while keeping sensitivity to the upper layers.

First of all, the ALTIUS payload will consist of three independent optical channels. Each of them has its own aperture, filter and sensor, and a specific spectral range: UV (250-450 nm), VIS (440-800 nm), NIR (900-1800 nm). Therefore, each channel control unit (CCU) is free from setting gains and integration times according to the radiometric levels experienced at any given wavelength.

For the UV and VIS channels, the company CAELESTE (Belgium) is currently developing an architecture based on high dynamic range (HDR) CMOS pixels. Their approach is twofold:

- two available full well (FW) capacitances (33 ke$^-$ and 330 ke$^-$) selectable row per row,
- the possibility to tune the integration time row-wise with the limitation of the profile being monotonic, i.e. the exponentially varying radiance profile could be reflected as such in the integration times settings.

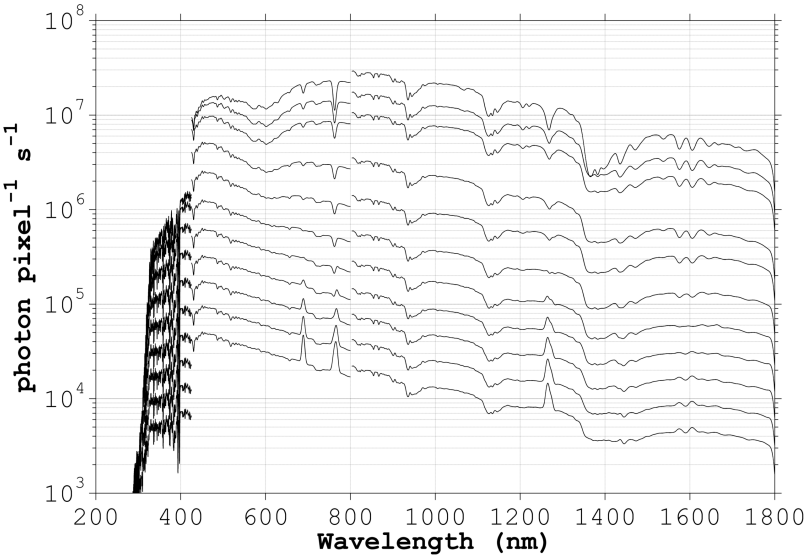

Figure 1. Radiative transfer model computation of the flux of photons per pixel in function of wavelength and tangent altitude. Each curve corresponds to one altitude starting from 10 km (top) up to 60 km (bottom) by steps of 5 km. The discontinuities at 440 nm and 800 nm owe to the different optical channels throughput. The radiance is convolved at the instrument nominal resolution (channel- and wavelength-dependent), but transmission losses and detection efficiency have been neglected.

With this concept, a bright limb spectral image would be recorded according to the following sequence. The acquisition starts with the upper rows (lowest signal) set with the small FW to minimize noise and programmed to collect photons during the longest allowed integration time ($\approx$1 s). Below a given row (i.e. tangent altitude), the stronger signal saturates the pixel before the end of acquisition, requiring to switch the bottom rows to the large FW. Saturation of the lowest rows is avoided by delaying their beginning of acquisition, i.e. the lowest rows will have a large full well and a shorter integration time. A similar design is used by CAELESTE in another project of HDR spectrometers. Prototyping activities have provided good results and confidence in the overall concept.

For the NIR channel, the commercially available space-qualified NEPTUNE HgCdTe detector from the SOFRADIR company equipped with a RICOR Stirling cooler has been selected. It does not provide a row-selectable integration time, but offers the two FW (520 ke$^-$ and 2.5 Me$^-$). Preliminary studies indicate that maintaining the chip temperature around 190 K will be sufficient to comply with the SNR requirements.

2.2 AOTF-based Hyperspectral Imager

The core-concept of ALTIUS is to mitigate the pointing uncertainties of a limb sounder by taking instantaneous spectral pictures of the limb. Obviously, the remote sensing of atmospheric species relies crucially on the identification of their spectral signature. Depending on the molecules, it is necessary to measure at several wavelengths with a relatively high spectral resolution. At the exception of an imaging Fourier transform spectrometer,[12] other suitable technologies take images at a single wavelength at a time. Acousto-optic tunable filter (AOTF) have some advantages over other options (dielectric filters, Fabry-Perot interferometers,...).

The AOTF is a small (a few cubic centimeters) robust device which contains no moving part and is made of a piezo-electric transducer bonded to a birefringent crystal. Here is a brief description of the working principle.[13] An acoustic wave is launched into the medium and induces local strains. These strains affect the electric susceptibility of the medium through the elasto-optic effect. In the presence of an electric field (incident light), a resonance can take place at a specific wavelength which is then diffracted into a slightly different direction (typical separation angle $< 10°$) with its polarization rotated by 90°. An instrument based on an AOTF has therefore the unique capability of being able to measure its own straylight: by switching the AOTF off (no diffracted beam), the acquired image only contains the parasitic light which can be later subtracted from the measurements. Compared to other filters, it is able to deliver narrower bandwidths ($<$ 1 nm-10 nm) while

Table 1. Main specifications of the ALTIUS VIS and UV channel breadboards.

Specifications	**VIS**	**UV**
Design	telecentric	telecentric
Entrance pupil diameter (mm)	8.73	5.24
Total focal length (mm)	125	128
Field of view (°)	5.7×5.7	2×2
AOTF aperture (mm)	10×10	10×10
Detector pixels array	512×512	512×512
Pixel size (μm)	24×24	24×24
Spectral range (nm)	400-800[a]	310-360[b]
Spectral resolution (nm)	0.6-3.5	0.5-0.7

[a]Limited by the tuning range of the transducer electrical matching network.
[b]Limited at shorter wavelengths by the transparency defect, and by the transducer electrical matching network at longer wavelengths.

preserving a non-negligible angular aperture (up to 10°). The tuning speed is of the order of a few μs (travelling time of the acoustic wave).

On ground, this technology is used in a broad range of hyperspectral applications (fluorescence or pattern detection, food quality control, microscopy,...). The most widespread material for the interaction medium is TeO_2 which possesses the highest acousto-optic figure of merit and is transparent from 0.35 to 5 μm. To our knowledge, no AOTF-based hyperspectral imager has been flown in a civil application. However, several instruments have used a TeO_2-based acousto-optic device, such as the SOIR instrument onboard Venus Express or earlier in the SPICAM instrument onboard Mars Express. Their long duration of nominal operation have *de facto* space qualified this technology.

Unfortunately, the transparency range of TeO_2 does not cover the needs for the UV channel such that another material must be found. Quartz is a birefringent crystal that is resistant and routinely used in UV optics, but its acousto-optic figure of merit is so low that the driving power would be much too large to achieve the required diffraction efficiency. Attempts have been made to use a KH_2PO_4 (KDP) crystal, a well-known material in nonlinear optics. We will further describe the developments related to the UV channel in Section 4.

3. PERFORMANCE OF A TEO2 AOTF-BASED VIS CHANNEL

In order to acquire practical knowledge with operating an AOTF-based hyperspectral imager, an optical breadboard of the ALTIUS VIS channel was built. It was designed and manufactured by OIP and BIRA-IASB, with a commercial TeO_2 AOTF purchased from the Gooch and Housego company (United Kingdom). Table 1 contains the main specifications. After characterization, it got a second life as a remote sensing instrument. One campaign led to the quantification of the NO_2 content in the plume released by a waste incinerator which has been the subject of a previous publication.[14] Further information can be found therein, such as the instrument description, more details on the AOTF principle, or sample spectral images.

Though not being its natural operational mode (as the acousto-optic interaction only occurs for one optical wavelength and one acoustic frequency at a time), an AOTF can also record continuous spectra, provided that acquisition time is not a constraint. By sweeping the acoustic wave frequency with reasonably small steps compared to the AOTF passband, one can record the diffracted beam intensity as a function of frequency. If the white incident light has been propagating through an absorptive medium, then a "continuous" absorption spectrum is obtained.

The rationale behind this experiment is that by looking at the structured absorption spectrum of a relevant species, it provides a measure of the spectral resolution of an AOTF-based remote sensing instrument. Second, it

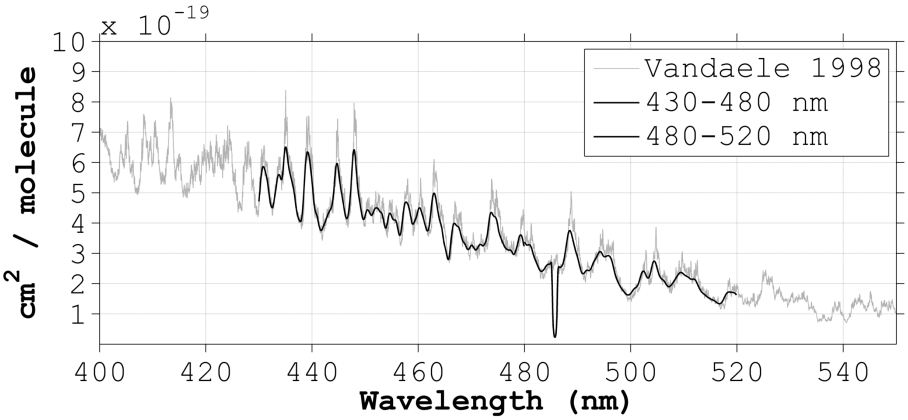

Figure 2. NO_2 absorption cross-section measured with the ALTIUS VIS channel breadboard and its TeO_2 AOTF (black curve) compared to a reference spectrum (grey curve).

is an excellent performance test for the tuning accuracy (how the driving electronics can be trusted) as hundreds of small steps are performed. Finally, it is one of the possible methods for the instrument wavelength scale calibration as the well-known spectral structures can serve as absolute references.

Among the family of atmospheric species, NO_2 is probably the best choice for this exercise: it plays an important role in the global ozone chemistry, it is relatively abundant in the stratosphere, and it presents a quite structured absorption spectrum[15] whose differential features are compatible with a moderate spectral resolution (about 1 nm).

For these reasons, we tested a TeO_2 AOTF in a laboratory experiment involving an absorption cell filled with NO_2. The measurements took place at the Katholieke Universiteit Leuven (KUL, Belgium), in the laboratory of the Quantum Chemistry and Physical Chemistry Section of the Chemistry department. A long-path absorption gas cell (120 cm long) was prepared and aligned with a deuterium lamp. A collimating lens was used to make the light beam parallel throughout the cell. The breadboard was collecting the light afterwards. The AOTF driving and the acquisition electronics were controlled by a LabView software.

The measurement strategy consisted of two steps. First, a reference measurement was recorded with the empty cell. Practically, the acoustic frequency was swept by steps corresponding to 0.1 nm in the wavelength space. At each step, the diffracted beam intensity was averaged over 0.5 seconds, then corrected for the background signal (straylight removal) and stored. After completion of this reference scan, the cell was filled with a mixture of He (95%) and NO_2 (5%) at 10 Torr and the same acquisition sequence was run.

The extinction of light by absorption from NO_2 follows the Beer-Lambert law: $I(\lambda) = I_0(\lambda)\,\exp(-\sigma(\lambda)\,L\,n)$. In this expression, $I(\lambda)$ and $I_0(\lambda)$ are the spectral intensity measured at the wavelength λ with and without absorption respectively, σ is the absorption cross-section that we want to measure, L is the absorption path length (the cell length), and n is the gas number density.

Fig. 2 shows the experimental data superimposed on the reference spectrum recorded with a Fourier transform spectrometer at a 0.1 cm^{-1} resolution.[15] The agreement is very good except around 486 nm, where the strong D_β emission line from the hydrogen Balmer series corrupted the data by saturating the detector (thus a lamp effect independent of the AOTF).

Clearly, a remote sensing instrument based on an AOTF showing similar specifications as the ALTIUS VIS channel breadboard allows to resolve the characteristic structures of the NO_2 absorption cross-section. As the measurement principle relied on a quite unusual way of operating the AOTF (hundreds of close steps), this was yet to be demonstrated.

4. PERFORMANCE OF A KDP AOTF-BASED UV CHANNEL

In 2004, Voloshinov and Gupta demonstrated that significant diffraction efficiency in the UV down to 200 nm could be obtained from a KDP AOTF with a wide angular aperture and reasonable driving power.[16,17] Due

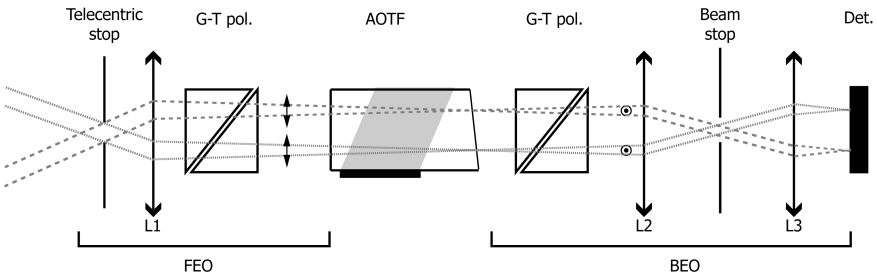

Figure 3. Schematic drawing of the ALTIUS UV channel breadboard seen from top. The KDP AOTF is surrounded by two cross-oriented Glan-Taylor polarizers to better remove the undiffracted order. The optical design is telecentric such that the Bragg condition of the acousto-optic diffraction is preserved over the entire aperture, i.e. to minimize any wavelength shift within the spectral image. The detector is a 512×512 pixels CCD camera from Princeton Instruments.

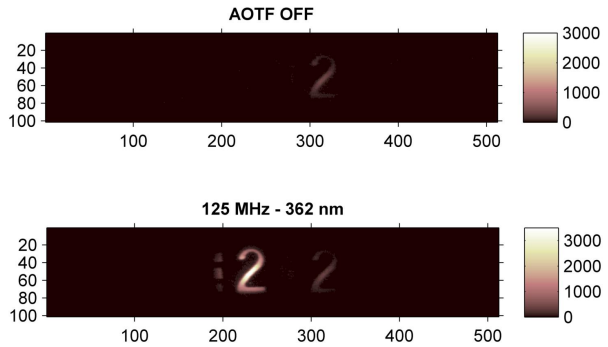

Figure 4. Top: Image acquired by the ALTIUS UV channel breadboard with the AOTF turned off. The weak signal forming the "2" shape comes from the strongly attenuated light beam which has passed two cross-oriented polarizers for zero-order suppression. The spectrum of the detected photons covers a 100 nm wide region defined by the bandpass filter inserted in the setup to limit the amount of light. Bottom: Spectral image captured with the AOTF driven by a 2W RF signal at 125 MHz. The signal is much more intense, though it is made of a narrow distribution of wavelengths around 362 nm. The residual image remains on the right side and can therefore be removed using the top image.

to the importance of UV measurements for an ozone mission, this breakthrough demonstration was the missing piece for a consistent instrumental concept: three independent channels operating in distinct spectral regions but relying on the same technology (AOTF) and optical design.

Through collaboration with the Moscow State University, a UV channel breadboard was manufactured (Fig. 3), hosting a KDP AOTF delivering nominal performance according to acousto-optic theory, but with degraded transparency properties: the cut-off wavelength was measured at 310 nm instead of 200 nm, probably due to metallic ion contamination during the crystal growing phase. The main specifications are given in Table 1

This breadboard was first used in spectral imaging tests. A deuterium lamp provided the UV light source illuminating a punched target (mask) showing straight parallel lines and numbers. A Schott UG-1 bandpass filter limited the spectrum to a window of roughly 100 nm width from 300 to 400 nm. A collimating lens of very short focal length made an intermediate image of the illuminated mask which was then captured by the breadboard.

Fig. 4 shows two frames acquired with the breadboard. The first one (top) was captured with the AOTF turned off. The pattern we see is the residual of the undiffracted beam strongly attenuated by the cross-oriented polarizers. The second frame has been acquired with the AOTF driven by a 2W RF signal at 125 MHz. In the wavelength domain, this frequency corresponds to 362 ± 0.35 nm. The spectral image appears with a much stronger intensity than the residual beam at some distance to the left of the undiffracted order due to the AOTF principle. Other pictures were acquired at smaller wavelengths down to 330 nm.

This simple experiment confirms that spectral images can be acquired with a KDP AOTF which shows

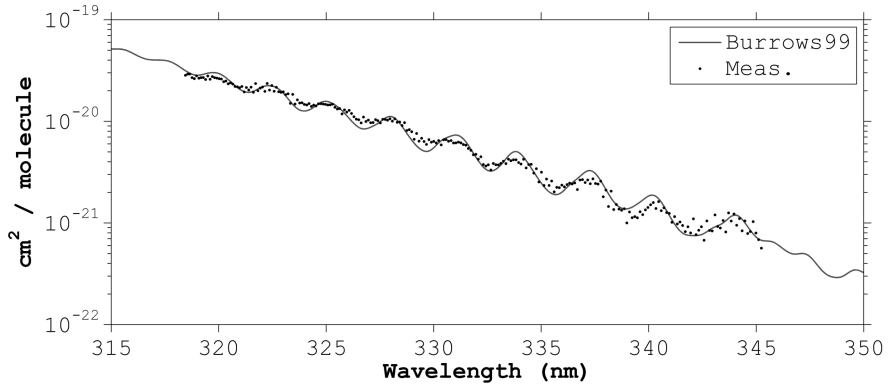

Figure 5. Huggins band structures of ozone captured by the ALTIUS UV channel breadboard and its KDP AOTF during a laboratory experiment with a static ozone cell (dots). The continuous line is the reference cross-section[19] convolved with a Gaussian function (FWHM = 0.7 nm).

sufficient diffraction efficiency and optical quality. It also illustrates one of the very interesting properties of the AOTF: it is a tunable spectral filter that truly separates the desired spectral image from the unwanted beam (angular separation and rotation of the polarization), and it can even be completely turned off. If the spectral image contains some residual light like in our example, this straylight can be captured alone (AOTF off) and then subtracted. This is definitely an important feature for a remote sensing instrument which other technologies do not possess.

Similarly to what was done with the VIS breadboard and the NO_2 cross-section, the spectral capabilities of the UV breadboard was tested in an experiment. The UV part of the ozone absorption cross-section is characterized by a maximum at 250 nm, and a minimum at 360 nm. In between, the Huggins band (320-360 nm) features smooth oscillations over multiple orders of magnitude. We tested the capability of the instrument to capture these structures by performing a spectral scan. Again, this is not a common way of operating an AOTF, but a good test case as it illustrates the spectral resolution and the stability of the device.

The experiment was carried out at the laboratory of molecular physics for atmosphere and astrophysics (LPMAA, now LERMA, Université Pierre et Marie Curie, Paris, France) using a dedicated ozone generation system.[18] Ozone was prepared and flushed into a static cell (30 cm long) until a concentration equivalent to a standard atmospheric column of 300 DU was reached. The light of a deuterium lamp was collimated through the cell and directed into the breadboard aperture. The measurements consisted of sweeping the driving RF by steps of 60 kHz (equivalent to 0.1 nm) while taking snapshots at each frequency. The sequence was repeated with an empty cell to provide the reference spectrum.

The results are shown in Fig. 5. The experiment proved that the instrument was capable of resolving the typical oscillations of the Huggins band over more than one order of magnitude. However, during the acquisition, the deuterium lamp became unstable and started behaving in a nonlinear way. The net result was that while the oscillations were well captured, the absolute cross-section could not be determined. The data points presented in Fig. 5 have simply been re-scaled to superimpose on the reference data such as to make the comparison easier.

5. CONCLUSION

ALTIUS is a small mission aiming at filling the forthcoming gap of atmospheric limb sounders by providing accurate ozone concentration profiles with high vertical resolution. Other species like NO_2, aerosols, PSC, PMC, H_2O or CH_4 are secondary targets. From a sunsynchronous LEO, ALTIUS will rely on two different measurement geometries: the limb-scattered sunlight on the dayside and solar, stellar, lunar and planetary occultations over the rest of the orbit. The needed manœuvrability and pointing precision will be provided by a PROBA platform.

In order to minimize the tangent altitude uncertainty, ALTIUS will take instantaneous snapshots of the limb in its three spectral channels in parallel (UV,VIS and NIR spanning 250-1800 nm). Compared to scanning spectrometers, the imaging capability brings new pointing calibration approaches such as bright star detection

in the background. This makes occultation measurements a lot easier, as the broad FOV alleviates the need for a sophisticated tracking system and makes inertial pointing feasible. Special developments have been undertaken at the detector level to deal with the high dynamic range of the bright limb. The UV and VIS detector architecture will provide two selectable full wells (on a row basis) and the capability of setting the integration time row per row.

The spectral information will be provided by an AOTF. Such device offers a number of advantages for a hyperspectral remote sensing instrument: tunable, fast, lightweight, no moving part, low power consumption,... Moreover, its working principle based on the spatial separation of the desired spectral content from the incident white light and on the rotation of the light polarization makes it very efficient at straylight removal.

Two optical breadboards have been manufactured, one for the UV and one for the VIS channel. Both include an AOTF (TeO_2 in the VIS, KDP in the UV). It has been demonstrated that the spectral resolution of such device is sufficient for capturing the spectral structures of two important atmospheric trace gases: O_3 and NO_2. Though operated in a very unconventional way (driving frequency swept over tens of nanometers), it gives confidence on the stability of the driving electronics at the transducer level and on its resistance to long-term operations.

ACKNOWLEDGMENTS

The authors would like to thankfully aknowledge the support from Pr. Shaun Carl and Dr. Victor Khamaganov for providing the test setup and assistance for the NO_2 absorption cross-section measurements. The ALTIUS project is supported by the Belgian Federal Science Policy Office (BELSPO) and funded through ESA-PRODEX contract PEA4200090274.

REFERENCES

1. WMO, *Scientific assessment of ozone depletion: 2010*, 2010.
2. A. E. Bourassa, D. A. Degenstein, W. J. Randel, J. M. Zawodny, E. Kyrölä, C. A. McLinden, S. E. Sioris, and C. Z. Roth, "Trends in stratospheric ozone derived from merged SAGE II and Odin-OSIRIS satellite observations," *Atmos. Chem. Phys.* **14**, pp. 6983–6994, 2014.
3. E. Kyrölä, M. Laine, V. Sofieva, J. Tamminen, S.-M. Pivrinta, S. Tukiainen, J. Zawodny, and L. Thomason, "Combined SAGE II-GOMOS ozone profile data set for 1984-2011 and trend analysis of the vertical distribution of ozone," *Atmos. Chem. Phys.* **13**, pp. 10645–10658, 2013.
4. C. Gebhardt, A. Rozanov, R. Hommel, M. Weber, H. Bovensmann, J. P. Burrows, D. Degenstein, L. Froidevaux, and A. M. Thompson, "Stratospheric ozone trends and variability as seen by SCIAMACHY from 2002 to 2012," *Atmos. Chem. Phys.* **14**, pp. 831–846, 2014.
5. E. Eckert, T. von Clarmann, M. Kiefer, G. P. Stiller, S. Lossow, N. Glatthor, D. A. Degenstein, L. Froidevaux, S. Godin-Beekmann, T. Leblanc, S. McDermid, M. Pastel, W. Steinbrecht, D. P. J. Swart, K. A. Walker, and P. F. Bernath, "Drift-corrected trends and periodic variations in MIPAS IMK/IAA ozone measurements," *Atmos. Chem. Phys.* **14**, pp. 2571–2589, 2014.
6. S. Tegtmeier and et al, "SPARC Data Initiative: A comparison of ozone climatologies from international satellite limb sounders," *J. Geophys. Res. Atmos.* **118**, pp. 12229–12247, 2013.
7. R. P. Loughman, D. E. Flittner, B. M. Herman, P. K. Barthia, E. Hilsenrath, and R. D. McPeters, "Description and sensitivity analysis of a limb scattering ozone retrieval algorithm," *J. Geophys. Res.* **110**, p. D19301, 2005.
8. J. Côté, A. Kron, J. de Lafontaine, J. Naudet, and S. Santandrea, "PROBA-2 Attitude and Orbit Control System: In-Flight Results of Innovative GNC Functions," *Proc. of the 18th IFAC World Congress* **18**, pp. 721–726, 2011.
9. D. F. Rault, "Ozone profile retrieval from Stratospheric Aerosol and Gas Experiment (SAGE III) limb scatter measurements," *J. Geophys. Res.* **110**, p. D09309, 2005.
10. G. Taha, G. Jaross, D. Fussen, F. Vanhellemont, E. Kyrölä, and R. D. McPeters, "Ozone profile retrieval from GOMOS limb scattering measurements," *J. Geophys. Res. Atmos.* **113**(D23), p. D23307, 2008.

11. G. Jaross, P. K. Bhartia, G. Chen, M. Kowitt, M. Haken, Z. Chen, P. Xu, J. Warner, and T. Kelly, "OMPS Limb Profiler instrument performance assessment," *J. Geophys. Res. Atmos.* **119**(7), pp. 4399–4412, 2014.
12. F. Friedl-Vallon and et al., "Instrument concept of the imaging Fourier transform spectrometer GLORIA," *Atmos. Meas. Tech. Discuss.* **7**, pp. 2301–2337, 2014.
13. J. Xu and R. Stroud, *Acousto-optic devices: principles, design, and applications*, Wiley series in pure and applied optics, Wiley, 1992.
14. E. Dekemper, N. Loodts, B. Van Opstal, J. Maes, F. Vanhellemont, N. Mateshvili, G. Franssens, D. Pieroux, C. Bingen, C. Robert, L. De Vos, L. Aballea, and D. Fussen, "Tunable acousto-optic spectral imager for atmospheric composition measurements in the visible spectral domain," *Appl. Opt.* **51**, pp. 6259–6267, 2012.
15. A. C. Vandaele, C. Hermans, P. C. Simon, M. Roozendael, J. M. Guilmot, M. Carleer, and R. Colin, "Fourier transform measurement of NO2 absorption cross-section in the visible range at room temperature," *J. Atmos. Chem.* **25**, pp. 289–305, 1996.
16. N. Gupta and V. Voloshinov, "Hyperspectral Imager, from Ultraviolet to Visible, with a KDP Acousto-Optic Tunable Filter," *Appl. Opt.* **43**, pp. 2752–2759, 2004.
17. V. Voloshinov and N. Gupta, "Ultraviolet-Visible Imaging Acousto-Optic Tunable Filters in KDP," *Appl. Opt.* **43**, pp. 3901–3909, 2004.
18. C. Janssen, D. Simone, and M. Guinet, "Preparation and accurate measurement of pure ozone," *Rev. Sci. Instr.* **82**, p. 034102, 2011.
19. J. P. Burrows, A. Richter, A. Dehn, B. Deters, S. Himmelmann, S. Voigt, and J. Orphal, "Atmospheric remote-sensing reference data from GOME-2. Temperature-dependent absorption cross sections of O3 in the 231–794 nm range," *J. Quant. Spectrosc. Ra.* **61**, pp. 509–517, 1999.